The Nature of Spin-State Transitions in Solid Complexes of Iron(II) and the Interpretation of Some Associated Phenomena

EDGAR KÖNIG,* GERHARD RITTER, and S. K. KULSHRESHTHA†

Institut für Physikalische und Theoretische Chemie and Physikalisches Institut, Abt. II, University of Erlangen-Nürnberg, D-8520 Erlangen, West Germany

Received January 7, 1985 (Revised Manuscript Received March 18, 1985)

Contents

I. Introduction

Spin-state transitions in various complexes of the transition-metal ions have received considerable attention within the last few years.[1-5] These transitions are encountered for metal ions characterized by the electronic configurations $3d^4$, $3d^5$, $3d^6$, and $3d^7$ in octahedral symmetry, if the cubic crystal-field splitting $\Delta = 10Dq$ and the Hund's rule exchange energy P are comparable in magnitude. For lower than octahedral symmetry, spin transitions have been found, in addition, for the configuration $3d^8$. In the particular case of $Fe^{2+}(3d^6)$ in octahedral symmetry, the relevant states are low spin $^1A_1(t_2^6)$, a singlet, and high spin $^5T_2(t_2^4e^2)$, with 15-fold degeneracy. The "crossover" condition then results as[6]

$$10Dq = 2.195B + 3.708C \quad (1)$$

where B and C are the Racah parameters of interelectronic repulsion. The quantity 10Dq at the crossover has been estimated to about 12 000 cm^{-1}.[7] In most real situations, the 15 levels of the $^5T_2$ state are split by spin-orbit interaction and lower symmetry crystal fields. The essential features of the high-spin($^5T_2$) ⇌ low-spin($^1A_1$) transition are not significantly altered, if the effective symmetry is lower than octahedral. The cubic designation of the states $^5T_2$ and $^1A_1$ will be therefore retained if $3d^6$ ions are concerned, whereas a spin transition without reference to a particular configuration will be denoted as HS ⇌ LS transition.

In dilute solution, where the molecules are effectively isolated, in general an equilibrium between the LS and HS states is established. The interconversion process is dynamic in nature and may be characterized by

$$LS \underset{k_{-1}}{\overset{k_1}{\rightleftharpoons}} HS \quad (2)$$

The rate constants for the process have been determined for a number of systems. For iron(II) complexes, in particular, the values obtained for k_1 and k_{-1} vary between 4×10^5 and 2×10^7 s^{-1}.[8]

In solid systems, thermally driven transitions between LS and HS states are observed, the behavior being modified, to different extents, by interactions within the lattice. There are two different types of spin transition which may be distinguished: (i) discontinuous (abrupt) transitions which occur at a well defined transition temperature (T_c); (ii) continuous (gradual) transitions which take place over an extended range of temperature (T_c defined by the temperature where the HS fraction $n_{HS} = 0.50$).

In order to provide an interpretation of spin-state transitions, a number of theoretical models has been conceived, reference being given here only to a few.[9-14] These studies seem to account rather well for the general observation that both discontinuous and continuous type of transition are encountered. In any particular model, the type of transition is determined by the specific numerical values which are assumed for certain parameters. Thus, in an Ising-type model,[10] an interaction term is introduced such that the energy of the HS and LS states of a given ion depends on the spin state of neighboring ions. For the $Fe^{2+}(3d^6)$ ion, e.g., the characteristic parameter is J/kT_c where J is the interaction constant for the $^5T_2$ ions and T_c is the transition temperature. A gradual transition then results for $J/kT_c < 2.0$, whereas abrupt transitions are obtained if $J/kT_c \geq 2.0$ (orbital splitting parameter $\Delta_1 = \Delta_2 = 500$ cm^{-1}, spin-orbit coupling constant $\lambda = -100$ cm^{-1} and $T_c = 150$ K assumed[10]). The results of the experimental studies are difficult to reconcile with this type of model. Thus, X-ray diffraction investigations clearly show the presence of two different phases for discontinuous transitions, whereas a single phase is indicated for continuous transitions (cf. section III for details). Obviously, it is not easy to account for the observation by the adjustment of a single model parameter.

In this situation, it seems profitable to present a short account of our current understanding of spin-state

†Permanent address: Chemistry Division, Bhabha Atomic Research Centre, Bombay 400 085, India.

0009-2665/85/0785-0219$06.50/0

Edgar König was born in Prague, Czechoslovakia, in 1929. He obtained his diploma in chemistry from the University of Frankfurt, West Germany, in 1957 and his Ph.D. in 1959. After postdoctoral work with H. L. Schläfer in Frankfurt, he joined Mellon Institute in Pittsburgh, PA, in 1962–1965. After 1 year as a guest at the H. C. Ørsted Institute with C. J. Ballhausen in Copenhagen, he joined the faculty of the University of Erlangen-Nuremberg, West Germany, where he is now Professor. His research interests are magnetism and spectroscopy of transition-metal complexes.

Gerhard Ritter was born near Eger, Czechoslovakia, in 1932. He obtained his diploma in physics from the University of Erlangen-Nuremberg, West Germany, in 1960 and his Ph.D. in 1965. After postdoctoral work with H. Wegener, he joined in 1973 the faculty of the University of Erlangen-Nuremberg where he is now Professor. His research interests are centered around Mössbauer spectroscopy.

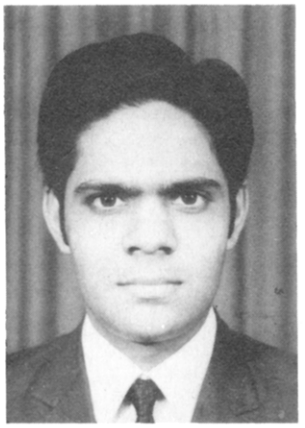

Shailendra K. Kulshreshtha was born in Aligarh, India, in 1947. He obtained his B.S. in physics from the University of Agra, India, in 1966 and his Ph.D. from the University of Bombay in 1973. In 1967 he joined the Bhabha Atomic Research Centre in Bombay, where he is now Scientific Officer. In 1981–1982 he was a visiting scientist at the University of Erlangen-Nuremberg, West Germany, where he was associated with E. König and G. Ritter. His current research interest is concerned with the application of Mössbauer spectroscopy to catalysis and coordination chemistry.

transitions. The emphasis is on the most completely investigated spin transition complexes of iron(II). Inclusive of the tabulated data, the review is comprehensive with respect to those iron(II) crossover systems which have been investigated by multiple-temperature single-crystal X-ray diffraction or the high-resolution X-ray powder diffraction method. It is only in these cases that a reliable differentiation between the two types of transition, i.e., discontinuous and continuous, can be achieved.

Spin-state transitions have been reported for certain solids such as perovskites,[15,16] and clusters[17] as well as for various biological materials.[18–20] It is expected that the interpretation of spin-state transitions in these systems will follow closely the arguments outlined in this report.

II. Thermodynamic Aspects

It may be useful to consider the basic facts of the thermodynamics of phase transitions. The relative stability of two different phases is determined by the difference in the Gibbs free energy

$$G = H - TS \tag{3}$$

where $H = U + pV$ is the enthalpy and U the internal energy of the system. At low temperatures, and provided the entropy S is finite, the contribution of the term TS to the free energy of a phase is negligible. Consequently, the condition of stability is decided by the difference in energy of the phases, the more stable state being the state of lower energy. In HS $\rightleftharpoons$ LS transitions, this is, in general, the LS state.[6,21] At the transition temperature T_c, the free energies of the two phases are equal, $\Delta G = G_{HS} - G_{LS} = 0$ and thus $\Delta H = T\Delta S$. At sufficiently high temperatures, the term TS in eq 3 will dominate and the stable phase will be that of greater entropy. In general, the high-temperature phase also shows a higher disorder than the low-temperature phase. The increase in entropy ΔS in a HS $\rightleftharpoons$ LS transition may be related to disorder as follows. The total increase in entropy consists of electronic and vibrational contributions

$$\Delta S = \Delta S_{el} + \Delta S_{vib,mol} + \Delta S_{vib,lat} \tag{4}$$

where we have separated ΔS_{vib} into contributions from intramolecular vibrations $\Delta S_{vib,mol}$ and those of intermolecular or lattice vibrations $\Delta S_{vib,lat}$. Rotational entropy ΔS_{rot} and configurational entropy ΔS_{conf} need not be considered for HS $\rightleftharpoons$ LS transitions, the latter being of importance only in situations where orientational disorder of a molecular subunit is encountered.[22,23] ΔS_{el} may contain contributions from both spin and orbital degeneracy. In the cases of interest, however, orbital degeneracy is most often removed and thus

$$\Delta S_{el} \simeq \Delta S_{el}^{spin} = R \ln (\omega_{HS}/\omega_{LS}) \tag{5}$$

where ω_{HS} and ω_{LS} are the number of spin configurations (i.e., spin multiplicity) for the HS and LS state, respectively. Thus, for compounds of iron(II) where the spin states involved are high-spin $^5T_2$ and low-spin $^1A_1$, $\Delta S_{el}^{spin} = R \ln 5 = 13.4$ J K^{-1} mol^{-1}. Measured values of the entropy change at HS $\rightleftharpoons$ LS transitions for complexes of iron(II) vary between about 48 and 86 J K^{-1} mol^{-1}, cf. Table I.[24–26] This is considerably more than the value expected for a change in spin state alone.

TABLE I. Results of Calorimetric and DSC Measurements on Solid Spin Transition Complexes of Iron(II)

compound[a]	T_c, K	ΔH, kJ mol^{-1}	ΔS, J K^{-1} mol^{-1}	method	ref
$[Fe(phen)_2(NCS)_2]$	176.29	8.60 ± 0.14	48.78 ± 0.71	cal	24
$[Fe(phen)_2(NCSe)_2]$	231.26	11.60 ± 0.44	51.22 ± 2.33	cal	24
$[Fe(bpy)_2(NCS)_2]$	212	10.1 ± 0.5	48 ± 4	DSC	26
$[Fe(phy)_2](ClO_4)_2$	244.6	15.7 ± 1	64 ± 4	DSC	25
$[Fe(phy)_2](BF_4)_2$	282	24.2 ± 1	86 ± 5	DSC	25

[a] Ligand abbreviations: phen = 1,10-phenanthroline, bpy = 2,2′-bipyridine, phy = 1,10-phenanthroline-2-carbaldehyde phenylhydrazone.

The difference has been attributed to the vibrational entropy term ΔS_{vib} which is always large if the transition is associated with a sizable change in volume. For HS $\rightleftharpoons$ LS transitions, such a volume change has been clearly established on the basis of X-ray diffraction.[27-30] A detailed analysis of the vibrational contributions ΔS_{vib} has been provided for the spin transition in $[Fe(phen)_2(NCS)_2]$ and $[Fe(phen)_2(NCSe)_2]$.[24] According to this study, about 50% of the vibrational entropy is due to metal–ligand stretching vibrations, another large contribution being assigned to the N–Fe–N deformations, whereas the contribution by lattice vibrations is considered as minor. It is evident that the driving force of a spin transition from the LS to the HS state is the gain in entropy which is provided in part by the change in total spin and by another part by the associated change in molecular configuration.

The thermodynamic classification of phase transitions may be based on the behavior of the Gibbs free energy and its derivatives. At the transition temperature, G itself remains continuous, since the two phases must have the same free energy. According to eq 3, it is

$$\begin{aligned} dG &= dU + pdV + Vdp - TdS - SdT \\ &= Vdp - SdT \end{aligned} \tag{6}$$

The first derivatives of G with respect to temperature T and pressure p thus are

$$\left(\frac{\partial G}{\partial T}\right)_p = -S$$

$$\left(\frac{\partial G}{\partial p}\right)_T = V \tag{7}$$

The second derivatives are readily obtained as

$$\left(\frac{\partial^2 G}{\partial T^2}\right)_p = -\left(\frac{\partial S}{\partial T}\right)_p = -\frac{C_p}{T}$$

$$\left(\frac{\partial^2 G}{\partial p^2}\right)_T = \left(\frac{\partial V}{\partial p}\right)_T = -V\beta \tag{8}$$

$$\left(\frac{\partial^2 G}{\partial p \partial T}\right) = \left(\frac{\partial V}{\partial T}\right)_p = V\alpha$$

Here, C_p is the heat capacity at constant pressure, α the isothermal expansivity and β the isothermal compressibility. According to Ehrenfest,[31] a transition is said to be of the same order as the derivative of G which shows a discontinuous change at the transition temperature. Thus, a transition is first order if a discontinuous change occurs in volume and entropy (cf. eq 7). Since $\Delta S_{trans} = \Delta H_{trans}/T \neq 0$, the transition is also characterized by a nonvanishing latent heat ΔH_{trans}. In a transition which is second order, heat capacity, isothermal compressibility, and isothermal expansivity show a discontinuous change (cf. eq 8). Transitions of third and higher order will involve additional differential quantities.

Whereas it is not always obvious to characterize a particular transformation as second order, the characteristics of first-order transitions, such as a discontinuous change of volume or entropy or the existence of a measurable latent heat, are more easily recognized. However, it should be noted that many real transformations are indeed of mixed order, showing characteristic properties of both first- and second-order transitions. Ubbelohde[32] has therefore classified transformations simply as thermodynamically discontinuous and continuous transitions.

Hysteresis is another important property of first-order transitions that may be employed in their identification. Hysteresis arises as a difference in the transition temperatures depending upon whether the transition is approached from low or high temperatures. Evidently, the transformation does not take place at the true critical temperature T_c where the free energies $G_{I,II} = G(p,T,n_{HS})$ of the two phases are exactly equal, but rather at a higher and lower temperature, usually denoted $T_c^{\uparrow}$ and $T_c^{\downarrow}$, respectively, with a metastable region between the two. There are two possible causes for the appearance of hysteresis:[32,33]

(i) A distribution of transition temperatures as result of the formation of domains. Due to superheating and supercooling effects, each particular domain will have different transition temperatures $T_{ci}^{\uparrow}$, $T_{ci}^{\downarrow}$, the observed hysteresis curve being a superposition of the individual curves for all domains i.

(ii) A distribution of nucleation rates due to the existence of kinetic barriers. The height of the barriers increases with the value of the volume change ΔV accompanying the transition. For positive ΔV, the nucleation of the product phase is associated with a compression in the forward direction and with tension in the reverse direction thus producing a difference in transition temperatures in the two directions.

In these cases, the Gibbs free energy has to be extended by including additional terms which represent the strain energy ϵ and the interfacial energy η.[32] The free energy for the two phases that coexist in the metastable region may now be written as

$$\begin{aligned} G_I &= G(p, T, \epsilon_{12}, \eta_{12}) \\ G_{II} &= G(p, T, \epsilon_{21}, \eta_{21}) \end{aligned} \tag{9}$$

and thus a different transition temperature will be obtained as result of the different direction of temperature change.

III. Structural Considerations

Although the thermodynamic classification of phase transitions is very fundamental, since it relates the order

TABLE II. Results of Multitemperature Single Crystal X-Ray Diffraction Studies on Spin-State Transitions in Complexes of Iron(II)

compound[a]	T, K	V, Å^3	Fe–L distance, Å	L–Fe–L angle, deg	n_{HS}	ref
$[Fe(2\text{-pic})_3]Cl_2 \cdot C_2H_5OH$	298	2485.2	2.195	75.4	1.00[43]	29
$P2_1/c$, $Z = 4$	150	2406.2	2.175	76.4	~0.90	
(T_c = 121.5 K)	90	2344.2	2.013	81.5	<0.04	
$[Fe(2\text{-pic})_3]Cl_2 \cdot CH_3OH$[b]	227	4782	2.198 (HS)	76.0	0.84	28
Pbna, $Z = 8$			2.09 (LS)	77.7		
($T_c \simeq$ 153 K)	199	4795	2.203 (HS)	75.7	0.82	
			2.06 (LS)	79.3		
	171	4715	2.190 (HS)	76.4	0.66	
			2.02 (LS)	80.7		
	148	4691	2.184 (HS)	76.6	0.39	
			2.011 (LS)	81.8		
	115	4617	2.016	81.61	0.04	
$[Fe(dppen)_2Cl_2] \cdot 2(CH_3)_2CO$	295	2689.4	2.584	77.6	1.00[23]	30
$P2_1/a$, $Z = 2$, $T_c \simeq$ 240 K	130	2492	2.301	81.8	~0.04	
$[Fe(4\text{-Ettr})_2(H_2O)_2]_3(CF_3SO_3)_6$[b]	300	4168.2	2.174		1.00	37
$P\bar{3}1c$, $Z = 2$, T_c = 203 K	105	3994.9	2.031		0	

[a] Ligand abbreviations: 2-pic = 2-picolylamine; dppen = *cis*-1,2-bis(diphenylphosphino)ethylene; 4-Ettr = 4-ethyl-1,2,4-triazole. [b] Resolution of both HS and LS molecules at intermediate temperatures accomplished.

of the transition with discontinuities in the derivatives of Gibbs free energy, it provides not more than a macroscopic description of the transitions. With the accumulation of knowledge concerning the structure of solids, the classification into structural categories becomes important. Thus, a geometrical picture of the microscopic changes associated with a transition may be obtained, because the product phase formed in the transition may be related to the parent phase in one of several ways. The detailed description of the various structural types of phase transitions, such as reconstructive, displacive, martensitic, order–disorder, and others will not be attempted here. For details, the interested reader is rather referred to the literature in this field.[34-36]

There are a number of X-ray structure investigations available which were performed at two or more temperatures on spin transition compounds of iron(II)[28-30,37] (cf. Table II). According to these studies, the largest structural change encountered always concerns the Fe–ligand bond length. Thus, on transition from the LS to the HS state, Fe–N distances increase up to about 0.18 Å. The largest Fe–ligand bond length change has been observed for Fe–P ligation, the corresponding increase being 0.28 Å.[30] Another significant change concerns the ligand–Fe–ligand bite angle for bidentate ligands which decreases for N–Fe–N ligation, on transition from the LS to the HS state, by up to 6°. There are, in general, additional changes in bond lengths and angles of the ligand which are different for different compounds. No breaking of bonds or the formation of new bonds or any other more pronounced modification of the lattice has been found. Thus, in all compounds, the topology of the linkage in the lattice is preserved, and the space group is the same for the LS as well as for the HS state. It should be noted that all the compounds studied according to Table II show HS $\rightleftharpoons$ LS transitions of the continuous type. The results do not immediately conform to any of the types of phase transformation encountered for the more simple, i.e., ionic or metallic, lattices. However, it is at least evident that the change of spin and the order of electronic energy levels at the HS $\rightleftharpoons$ LS transition is associated with a geometric distortion of the molecular structure. It follows that the HS $\rightleftharpoons$ LS transitions may be considered as of the pure displacive type showing a similarity to the cooperative pseudo-Jahn–Teller transformations.

Multitemperature X-ray structure determinations have been also reported for various spin transition compounds of iron(III).[38-41] In general, the changes associated with the HS $\rightleftharpoons$ LS transition are closely similar to those in complexes of iron(II). Thus, e.g., in tris(dithiocarbamato)iron(III) complexes,[38,39] the change of Fe–S distances is only about 0.07 Å, and the change of the S–Fe–S bite angle is about 1.6°. In a particular porphinatoiron(III) complex,[40] the structural change on transition from the LS to the HS state can be described as an increase by 0.27 Å in the axial Fe–N bond and a porphinato ring expansion causing an increase of ~ 0.055 Å in the equatorial Fe–N bond. We assume, therefore, that the changes observed in HS $\rightleftharpoons$ LS transitions of iron(II) compounds are largely typical for spin transitions in general.

Despite the available structural information on spin transitions, the assignment of a particular spin transition to one of the two categories of discontinuous and continuous transitions is often not obvious on the basis of magnetic, spectroscopic, and Mössbauer effect measurements alone. It is therefore of some interest that a novel method for a reliable separation of the two types of transition has been developed. The method uses high-resolution X-ray powder diffraction which is studied as a function of temperature, and the analysis of the resulting peak profiles.[42] It has been demonstrated that, for discontinuous spin transitions, individual diffraction peaks for the two phases are observed. These signals replace each other as the transition progresses in either direction. For continuous transitions, diffraction peaks of a single phase are obtained. The position of these signals gradually shifts with temperature from the original position of the parent phase to that of the product phase in either direction.

In the following sections, we will review the available experimental results for spin transition compounds of iron(II). The examples have been such chosen that a detailed analysis of high-resolution X-ray powder diffraction or the single-crystal X-ray structure for the two phases, HS and LS, is available. On this basis, a reliable assignment of the spin transitions to the discontinuous or the continuous type has been possible in most cases.

IV. Discontinuous Transitions

A. Background

The discontinuous type of spin transition may be described in detail in terms of an abrupt change with temperature of important physical properties, such as the high-spin fraction n_{HS} derived on the basis of the ^{57}Fe Mössbauer effect, the relative intensity I_{HS}/I_{total} obtained from X-ray diffraction,[42] the effective magnetic moment μ_{eff}, and others. A characteristic transition temperature T_c exists or may be defined by that temperature where $n_{HS} = 0.50$. Experimentally, a compelling evidence for a crystallographic phase change is provided by the observation of individual X-ray diffraction patterns for the two ground states of iron(II), high-spin $^5T_2$ and low-spin $^1A_1$. In the region of T_c, the relative intensity I_{rel} of the two patterns is strongly temperature dependent and I_{HS}/I_{total} conforms to the temperature variation of n_{HS}. The first-order character of the transition often may be established from the measurement of heat capacity changes, from DSC studies or the observation of hysteresis effects.

Hysteresis effects are closely associated with the formation of domains and the mechanism of a spin transition may be characterized more completely by application of the Everett model[44-47] to the observed hysteresis. This model considers the behavior of an ensemble of domains as a function of an independent variable. In case of a spin transition, a domain is formed by a number of molecules of like spin, either high-spin (HS) or low-spin (LS). The conversion from one state to the other is effected by change of the independent variable, e.g., the temperature T. If the LS state is stable at low values of T, then on increasing T a change to the HS state will take place at the critical temperature $T_c^{\uparrow} = T$ (LS → HS), while the reverse change will occur on lowering T at the value $T_c^{\downarrow} = T$ (HS → LS) which is smaller than $T_c^{\uparrow}$. In general, the values of T_c will be different for different domains i, and are thus denoted $T_{ci}^{\uparrow}$, $T_{ci}^{\downarrow}$. The overall shape of the hysteresis for an observed physical quantity such as n_{HS} arises from the superposition of the individual hysteresis curves for a large number of domains i. Of particular interest is the distribution of the critical temperatures $T_{ci}^{\uparrow}$ and $T_{ci}^{\downarrow}$ which is determined by the distribution functions $p'(T^{\uparrow}) = dn_{HS}/d\vec{T}$ for the ascending boundary curve and $q'(T^{\downarrow}) = dn_{HS}/d\vec{T}$ for the descending boundary curve of the hysteresis.[44,46] It follows that rather abrupt transitions will be characteristic for a narrow distribution of critical temperatures $T_{ci}^{\uparrow}$, $T_{ci}^{\downarrow}$, whereas a more gradual character will be indicative of a wider distribution of $T_{ci}^{\uparrow}$, $T_{ci}^{\downarrow}$ for the individual domains. Since spin transition characteristics are very sensitive to changes in crystal properties, it is realistic to associate different slopes of hysteresis curves with such changes.

Valuable conclusions concerning the participation of domains in spin transitions may be drawn from the application of several theorems of the Everett model to inner loops of the hysteresis, the so-called "scanning curves".[44] Of particular importance is theorem 4 according to which the shape and area of scanning curves between two temperatures T_A and T_B should be equal independent of the position of A in the loop. This theorem as well as theorem 3 of Everett are valid only if the domains are independent.[47] It is customary to consider theorem 4, in particular, as the key theorem within a model of noninteracting domains.

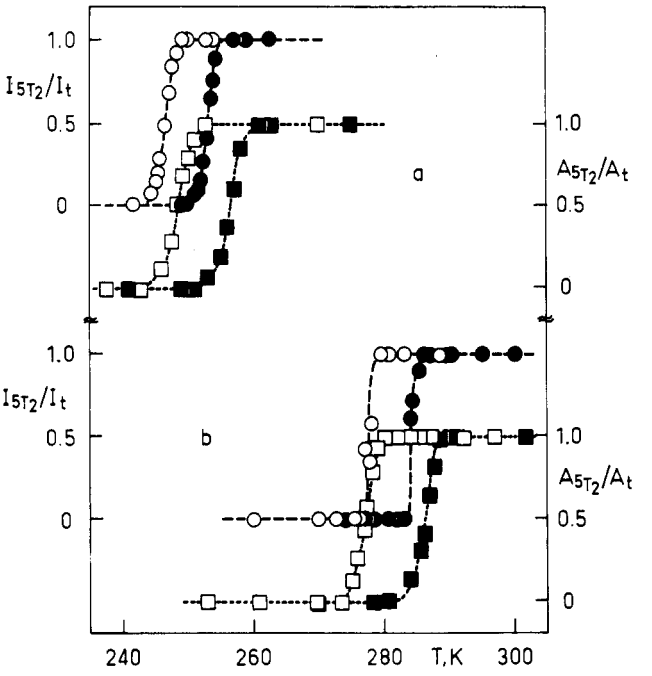

Figure 1. Temperature dependence of the high-spin area ratio A_{5T_2}/A_{total} on the basis of Mössbauer effect (□,■) and the relative intensity of the high-spin phase I_{5T_2}/I_{total} on the basis of X-ray diffraction (○,●) for $[Fe(phy)_2](ClO_4)_2$ (upper part of figure, a) and $[Fe(phy)_2](BF_4)_2$ (lower part of figure, b). Full points are for increasing temperatures; open points are for decreasing temperatures.

Discontinuous HS ⇌ LS transitions may arise for any transition-metal spin crossover system, although by far the largest number of known examples are complexes of iron(II) with various types of ligands.

B. Specific Examples

$[F(phy)_2][(ClO_4)_2$. The iron(II) complex of the tridentate ligand derived by a suitable substitution of 1,,10-phenanthroline in the 2-position (phy = 1,10-phenanthroline-2-carbaldehyde phenylhydrazone) shows an abrupt high-spin($^5T_2$) ⇌ low-spin($^1A_1$) transition.[48] The behavior of the ^{57}Fe Mössbauer effect is closely similar to that of the corresponding tetrafluoroborate which is discussed below. The transition is centered at $T_c^{\uparrow} = 256.1$ K for increasing and at $T_c^{\downarrow} = 248.0$ K for decreasing temperatures with a hysteresis of $\Delta T_c = 8.1$ K (cf. Figure 1). The recoil-free fraction shows a discontinuity of $\Delta f_{total} \simeq 42\%$ at $T_c^{\uparrow}$ as demonstrated by Figure 2 which indicates different phonon spectra for the two spin states. The enthalpy and entropy change at the transition have been determined by DSC measurements as $\Delta H = 15.7 \pm 1$ kJ mol^{-1} and $\Delta S = 64 \pm 4$ J K^{-1} mol^{-1}, respectively.[25] A distinct difference is found for the X-ray diffraction patterns of the two phases, HS and LS, cf. Figure 3. The transition temperatures for the crystallographic phase change ($T_c^{\uparrow} = 253.1$ K, $T_c^{\downarrow} = 246.5$ K) are practically identical to the values derived from Mössbauer effect, the differences being due to the experimental uncertainty of these values. This applies similarly to the

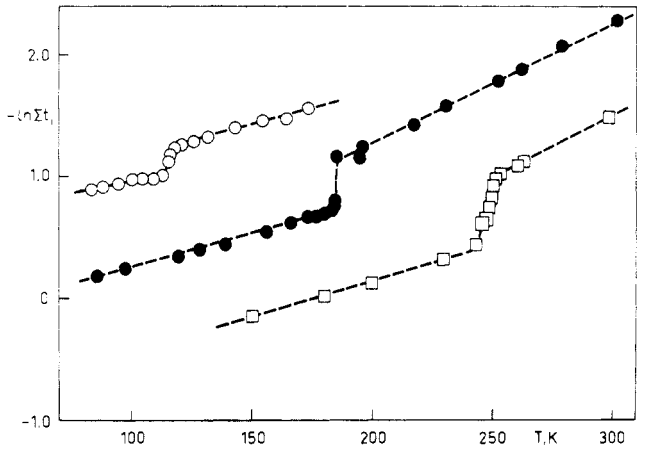

Figure 2. Temperature dependence of the quantity $-\ln(\sum t_i)$, $i = {}^5T_2$, $^1A_1$, where t_i is the effective thickness, on the basis of ^{57}Fe Mössbauer effect measurements for $[Fe(bi)_3](ClO_4)_2$ (○), $[Fe(bt)_2(NCS)_2]$ (●), and $[Fe(phy)_2](ClO_4)_2$ (□). The measurements are for increasing temperatures.

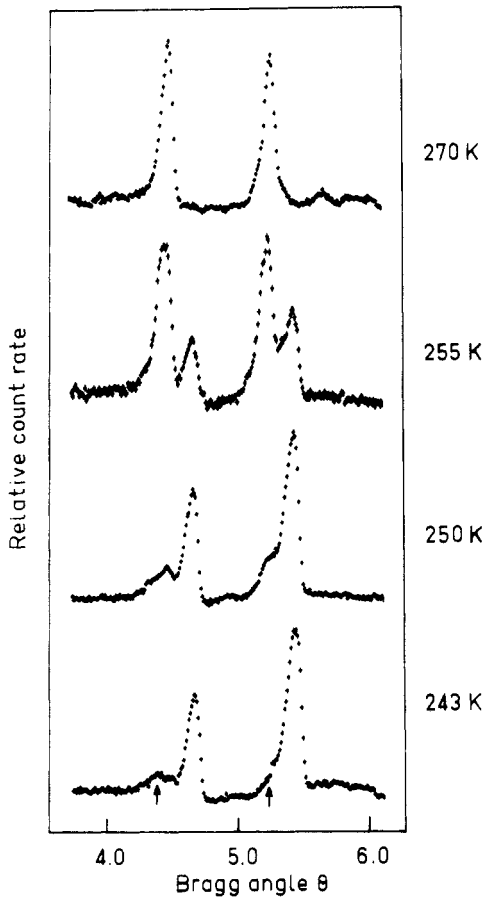

Figure 3. X-ray powder diffraction peak profiles for $[Fe(phy)_2](ClO_4)_2$ at the temperatures of 243, 250, 255, and 270 K. The measurements have been performed for increasing temperatures. Arrows mark the residual $^5T_2$ fraction (T_c = 253.1 K).

hysteresis curve derived from the relative intensities $I_{^5T_2}/I_{total}$ of X-ray diffraction where ΔT_c = 6.6 K (cf. Figure 1). The close correspondence between these data demonstrates that the electronic state of the molecules within the solid compound changes simultaneously with the crystallographic properties of the lattice. In order to determine whether independent domains are participating in the transition, two scanning curves of the hysteresis were constructed on the basis of X-ray diffraction measurements. These curves are displayed in Figure 4, the temperature of turning points being equal to within ±0.2 K.[49] The hatched areas in Figure 4 which are bound by the two inner loops have been determined by integration of areas and were found to be equal within 3%. On the basis of theorem 4 of the Everett model,[44] the results are consistent with the formation of independent domains by both the majority and minority phases of the two spin states, $^5T_2$ and $^1A_1$. The spin transition in the compound $[Fe(phy)_2](ClO_4)_2$ thus occurs by conversion of the domains of HS ($^5T_2$) molecules into domains of LS ($^1A_1$) molecules and vice versa.

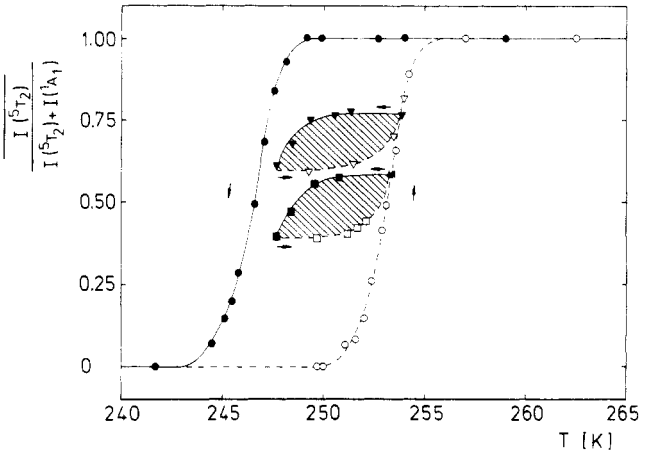

Figure 4. Temperature dependence of the relative intensity of X-ray diffraction $I_{^5T_2}/I_{total}$ for $[Fe(phy)_2](ClO_4)_2$ including two inner loops of the hysteresis curve ($T_c^{\uparrow}$ = 253.1 K, $T_c^{\downarrow}$ = 246.5 K).

$[Fe(phy)_2](BF_4)_2$. For the complex tetrafluoroborate, the temperature dependence of the ^{57}Fe Mössbauer effect is displayed in Figure 5. The high-spin($^5T_2$) ⇌ low-spin($^1A_1$) transition is again abrupt, although it takes place at a somewhat higher temperature than in the perchlorate, i.e., at $T_c^{\uparrow} \simeq 284$ K for increasing and at $T_c^{\downarrow} \simeq 277$ K for decreasing temperatures, the hysteresis showing a width ΔT_c = 7 K (cf. Figure 1).[51] A pronounced discontinuity in the total area of Mössbauer absorption is found at T_c which is due to the difference in the recoil-free fraction of $\Delta f_{total} \simeq 65\%$. The enthalpy and entropy change associated with the transition have been determined from DSC as $\Delta H = 24.2 \pm 1.0$ kJ mol^{-1} and $\Delta S = 85.8 \pm 4.0$ J K^{-1} mol^{-1}, respectively.[25,51] X-ray diffraction patterns for the two phases again show characteristic differences and the behavior in the region of T_c is similar to that of the perchlorate. The transition temperature ($T_c^{\uparrow} \simeq 284$ K, $T_c^{\downarrow} \simeq 277$ K) and the shape of the hysteresis curve based on values of $I_{^5T_2}/I_{total}$ are practically identical to those determined from Mössbauer spectra (cf. Figure 1). The determination of inner loops of the hysteresis curve indicates formation of independent domains.[52] The transformation HS ⇌ LS may be similarly induced by the application of a moderate pressure.[51,53]

$[Fe(4,7\text{-}(CH_3)_2\text{-}phen)_2(NCS)_2]$. This compound provided the first example for hysteresis effects associated with a HS ⇌ LS transition (phen = 1,10-phenanthroline).[54,55] The transition temperatures, based on studies of the ^{57}Fe Mössbauer effect, are $T_c^{\uparrow}$ = 121.7 K, $T_c^{\downarrow}$ = 118.6 K thus resulting in a hysteresis width of ΔT_c = 3.1 K. An inner loop of the hysteresis

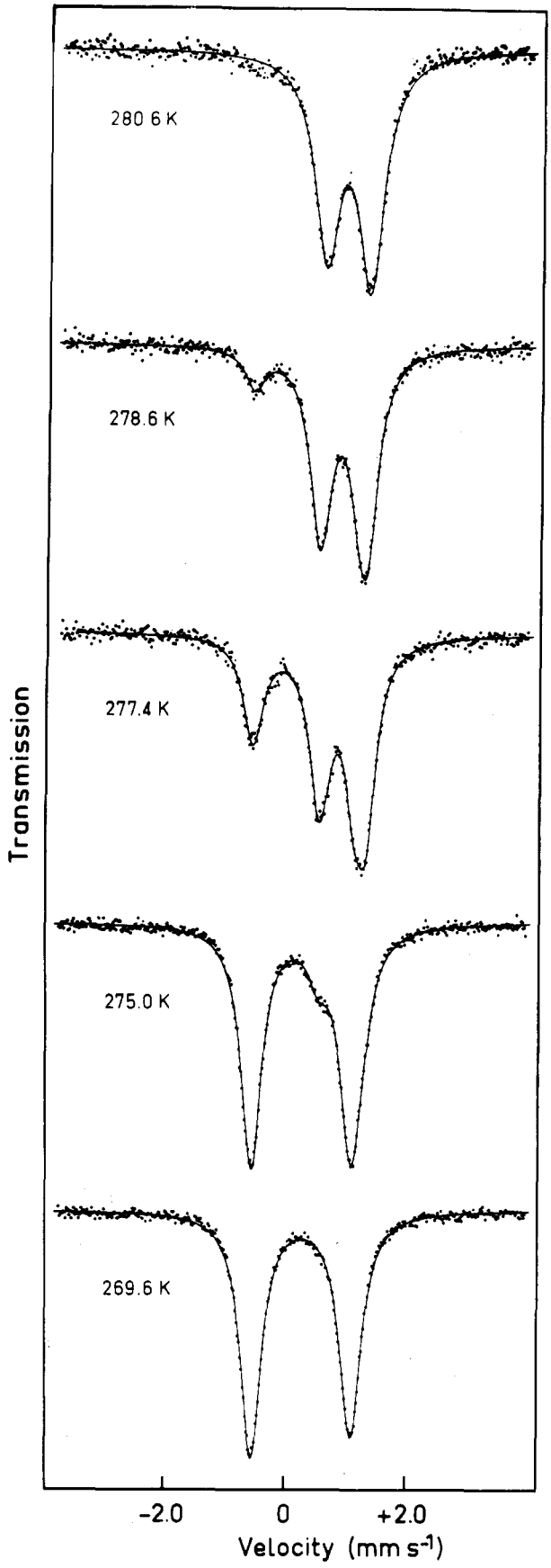

Figure 5. ^{57}Fe Mössbauer effect of $[Fe(phy)_2](BF_4)_2$ at 269.6, 275.0, 277.4, 278.6, and 280.6 K. The measurements were performed for decreasing temperatures ($T_c^{\downarrow} \simeq 277$ K).

curve was constructed, the results being consistent with the Everett model.[44] A clear discontinuity of the De-

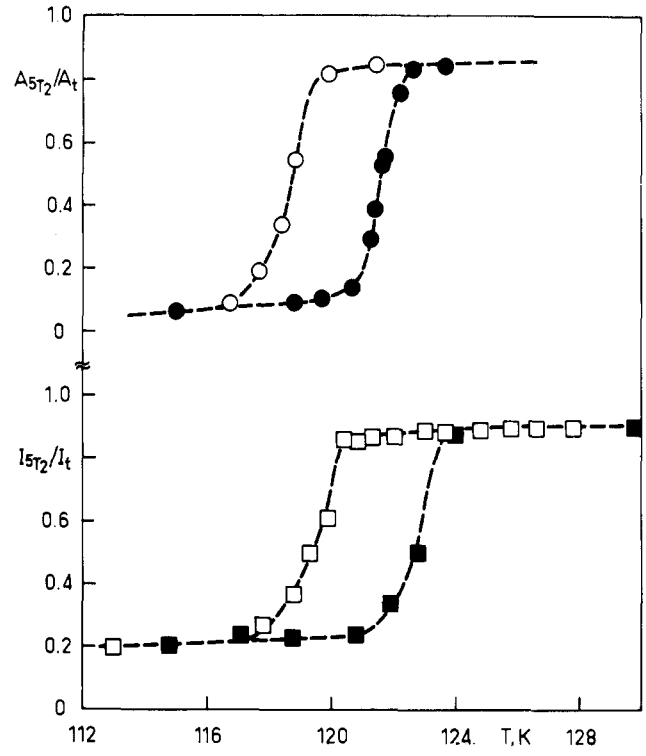

Figure 6. Temperature dependence of the high-spin area ratio $A_{^5T_2}/A_{total}$ on the basis of Mössbauer effect (○,●) and the relative intensity of the high-spin phase $I_{^5T_2}/I_{total}$ on the basis of X-ray diffraction (□,■) for $[Fe(4,7\text{-}(CH_3)_2\text{-phen})_2(NCS)_2]$. Full signs are for increasing temperatures; open signs are for decreasing temperatures.

bye–Waller factor was observed at T_c which is equivalent to $f_{^5T_2}$ being by 17% lower than $f_{^1A_1}$. The finding confirms the expected difference in lattice vibrations for the two spin-state phases.[56] X-ray diffraction produced different peak profiles for the two phases.[55] The relative intensity $I_{^5T_2}/I_{total}$ derived therefrom conforms closely to the area ratio $A_{^5T_2}/A_{total}$ derived from Mössbauer spectra (cf. Figure 6). Transition temperatures ($T_c^{\uparrow}$ = 122.9 K, $T_c^{\downarrow}$ = 119.6 K) are also in good agreement with those determined by other types of physical measurement. Similar results have been obtained for the α-picoline solvate of the compound which is of interest for its large hysteresis width ΔT_c = 56 K.[57]

[Fe(phen)$_2$(NCS)$_2$]. For the classical spin transition complex of the unsubstituted 1,10-phenanthroline ligand, a sharp transition was reported[58] at T_c = 174 K on the basis of magnetic and ^{57}Fe Mössbauer effect studies. The first-order character of the transition was confirmed by heat capacity measurements resulting in ΔH = 8.60 ± 0.14 kJ mol^{-1} and ΔS = 48.78 ± 0.71 J K^{-1} mol^{-1} at T_c = 176.29 K.[24] It was suggested that a long range correlation should be responsible for the cooperative nature of the transition through coupling between the electronic states of the complexes and the phonon system. X-ray powder diffraction peak profiles were studied over an extended range of temperature.[59] Only small changes of the diffraction pattern were apparent as compared to other spin transitions of the discontinuous type. It was concluded that the structural characteristics of the $^5T_2$ and $^1A_1$ phase should be closely related.[59] Recently, a very narrow hysteresis of the width ΔT_c = 0.15 K has been detected[60] by magnetic measurements, again suggesting that the structural change associated with the spin transition must be

TABLE III. Hysteresis Effects at Discontinuous Spin Transitions in Compounds of Iron(II)

compound[a]	$T_c^{\uparrow}$, K	$T_c^{\downarrow}$, K	ΔT_c, K	$\bar{T}_c$, K	method[b]	ref
$[Fe(bi)_3](ClO_4)_2$	114.8	108.3	6.5	111.6	X-ray	22
$[Fe(bt)_2(NCS)_2]$	181.9	172.3	9.3	177.1	X-ray	63
$[Fe(bpy)_2(NCS)_2]$	212.6	212.2	0.4	212.4	DSC	60
$[Fe(phen)_2(NCS)_2]$ extracted	176.30	176.15	0.15	176.23	cal	60
$[Fe(4,7\text{-}(CH_3)_2\text{-}phen)_2(NCS)_2]\cdot$	121.7	118.6	3.1	120.2	X-ray	54
α-picoline powdered	202	146	56	174	X-ray	57
α-picoline crystalline	195	153	42	174	X-ray	57
$[Fe(phy)_2](ClO_4)_2$	256.1	248.0	8.1	252.1	DSC, X-ray	48
$[Fe(phy)_2](BF_4)_2$	286	277	~9	281.5	DSC, X-ray	51
$[Fe(paptH)_2](NO_3)_2$	263	229	34	246		66
$[Fe(2\text{-}pic)_3]Cl_2\cdot H_2O$	295	204	~90	249.5		65

[a] Ligand abbreviations: bi = 2,2′-bi-2-imidazoline; bt = 2,2′-bi-2-thiazoline; bpy = 2,2′-bipyridine; phen = 1,10-phenanthroline; phy = 1,10-phenanthroline-2-carbaldehyde phenylhydrazone; paptH = 2-(2-pyridylamino)-4-(2-pyridyl)thiazole; 2-pic = 2-picolylamine. [b] Method employed to establish first-order character of transition: cal = calorimetry, DSC = differential scanning calorimetry, X-ray = X-ray diffraction.

small. The results for the analogous compound $[Fe(phen)_2(NCSe)_2]$ where $T_c = 232$ K are in many respects very similar.[24,58]

$[Fe(bpy)_2(NCS)_2]$. The complex of bpy = 2,2′-bipyridine shows a sharp transition at $T_c = 212$ K on the basis of magnetic and ^{57}Fe Mössbauer effect studies.[61] The first-order character of the transition is established by a discontinuous change of entropy and the observation of hysteresis effects. Thus, from DSC studies, $\Delta H = 10.1 \pm 5$ kJ mol^{-1} and $\Delta S = 48 \pm 4$ J K^{-1} mol^{-1} have been obtained;[26] whereas a very narrow hysteresis of the width $\Delta T_c = 0.4$ K has been found on the basis of magnetic measurements.[60] Of considerable interest are single crystal X-ray diffraction studies at 295 and ~100 K on polymorph II of the compound.[27] According to this study, the compound crystallizes in space group *Pcnb* with $Z = 4$. The average Fe–N bond length is 2.14 Å in the HS state and 2.02 Å in the LS state, thus showing an increase by 0.12 Å on transition from the LS to the HS state. Pronounced changes are also found for the N–Fe–N bond angles.

$[Fe(bt)_2(NCS)_2]$. The complex of another bidentate NN ligand (bt = 2,2′-bi-2-thiazoline) shows an abrupt high-spin($^5T_2$) ⇌ low-spin($^1A_1$) transition at $T_c^{\uparrow} = 181.9$ K and $T_c^{\downarrow} = 172.3$ K.[62,63] The hysteresis assumes a width of $\Delta T_c = 9.3$ K, a discontinuity of the recoil-free fraction of $\Delta f_{total} \simeq 35.4\%$ being observed at $T_c^{\uparrow}$. X-ray diffraction studies show significant differences for the HS and LS phases, the temperature dependence of the relative intensities $I_{^5T_2}/I_{total}$ being equivalent to that of the effective thickness $t_{^5T_2}/t_{total}$ derived from the Mössbauer effect. More recently, two inner loops of the hysteresis curve were constructed on the basis of magnetic measurements.[50] The areas of the loops were found to be equal except for a difference of 4 ± 1%. It was concluded that independent domains of molecules with like spin are participating in the spin transition.

$[Fe(bi)_3](ClO_4)_2$. In this complex where bi = 2,2′-bi-2-imidazoline,[64] a very sharp high-spin($^5T_2$) ⇌ low-spin($^1A_1$) transition was established by variable-temperature ^{57}Fe Mössbauer effect ($T_c^{\uparrow} = 114.8$ K, $T_c^{\downarrow} = 108.3$ K) and X-ray diffraction measurements.[22] Thus, a pronounced hysteresis of $\Delta T_c = 6.5$ K is observed, the recoil-free fraction showing a difference of $\Delta f_{total} \simeq 14\%$ at T_c (cf. Figure 2). Again, characteristically different X-ray diffraction patterns for the $^5T_2$ and $^1A_1$ phases are observed. At higher temperatures, the behavior of the compound becomes more complicated in that, at $T_c^{ClO_4} \simeq 199$ K, an order–disorder transition of the ClO_4 anions is involved.

C. Additional Comments

There are a few more iron(II) compounds for which a discontinuous type high-spin($^5T_2$) ⇌ low-spin($^1A_1$) transition has been reported. For these systems, the particular results which are required for a more detailed characterization of the transition are, in general, not available. $[Fe(2\text{-}pic)_3]Cl_2\cdot H_2O$ is of some interest for its extremely wide hysteresis of $\Delta T_c \simeq 90$ K (2-pic = 2-picolylamine). The transition temperatures were determined by a study of the ^{57}Fe Mössbauer effect, values of $T_c^{\uparrow} = 295$ K for increasing and $T_c^{\downarrow} = 204$ K for decreasing temperatures having been obtained.[65] Although the observation of hysteresis is indicating a first-order transition, an X-ray diffraction study is not available to ascertain the expected crystallographic phase change. Another example of an observed hysteresis is the transition in $[Fe(paptH)_2](NO_3)_2$ which shows a quasi-continuous appearance (paptH = 2-(2-pyridylamino)-4-(2-pyridyl)thiazole).[66] The transition temperatures were determined on the basis of the ^{57}Fe Mössbauer effect as $T_c^{\uparrow} = 263$ K, $T_c^{\downarrow} = 229$ K, the hysteresis width thus being $\Delta T_c = 34$ K. An X-ray diffraction investigation on the compound is in progress. The results of the more detailed hysteresis measurements on spin transitions in iron(II) complexes are collected in Table III.

Discontinuous type spin transitions have been also observed for compounds of other transition metals. An interesting example is the Schiff base complex [Fe(salen)NO] where an abrupt spin transition between $S = {}^3/_2$ and $S = {}^1/_2$ states has been observed at $T_c = 175 \pm 3$ K (salen = *N,N′*-ethylenebis(salicylideneamine)).[67] A hysteresis of $\Delta T_c \simeq 10$ K indicates that the transition is first order. Moreover, the temperature dependence of the Mössbauer total area shows a discontinuity at T_c. Fitting an Einstein model for local frequencies of vibration to the measured absorption areas it was concluded that there is a difference of ≃20% in the iron atom frequencies for the two spin phases. In a preceding study,[41] significant distortions and changes of the complex were found on the basis of single crystal X-ray diffraction at 296 and 98 K. The most striking changes observed for the $S = {}^1/_2$ phase are those of the Fe–N–O angle (127° vs. 147° in the $S = {}^3/_2$ state), the distance of the Fe atom to the mean coordination plane which is 0.1 Å lower, and the near coplanarity of the salen moieties.

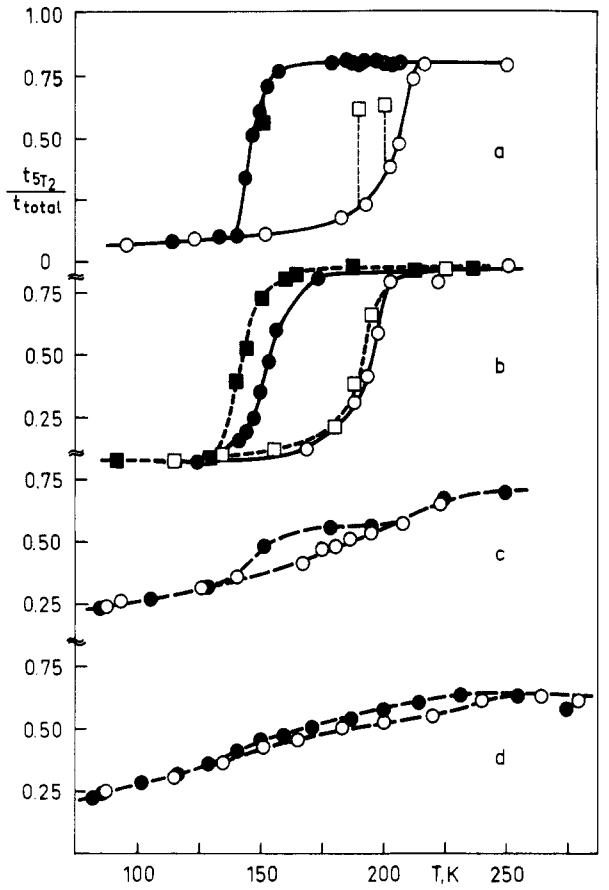

Figure 7. Temperature dependence of the relative effective thickness t_{5T_2}/t_{total} for [Fe(4,7-$(CH_3)_2$-phen)$_2$(NCS)$_2$]·α-picoline. Data collected with increasing temperature are marked with open signs; those obtained with decreasing temperature are marked with full signs. (a) Mildly powdered sample. (b) Crystalline sample (two sets of measurements recorded within six months are shown). (c) Substance thoroughly ground with sintered MgO powder. (d) Same sample as (c), measurement after two months.

D. Particle Size Effects, Grinding and Dilution Experiments

The experimental characterization of discontinuous transitions is by no means trivial, since local nonuniformities and stresses, whether due to defects within or grain boundaries between crystals, may "smear out" a truly discontinuous transition over a finite temperature range. This may be illustrated by some observations on [Fe(phy)$_2$](ClO$_4$)$_2$ where the results reported above apply to a particular sample of the compound, i.e., sample I. In a subsequent measurement of the finely divided sample II, by the ^{57}Fe Mössbauer effect, a quasi-continuous transition with a relatively narrow hysteresis loop ($T_c^{\uparrow}$ = 262.8 K, $T_c^{\downarrow}$ = 260.0 K, width ΔT_c = 2.8 K) was obtained.[48] The temperature dependence of I_{5T_2}/I_{total} derived from the X-ray diffraction measurements produced a hysteresis curve practically identical to that obtained on the basis of ^{57}Fe Mössbauer effect. It should be noted that the essential features of the first-order transition, such as hysteresis and the separate X-ray diffraction patterns for the two phases, were preserved. After recrystallization, a discontinuous behavior of the transition associated with a hysteresis curve practically identical to that of sample I was assumed. There is a clear difference of behavior as compared to the continuous transitions discussed in section V below.

Similar observations have been reported for grinding and dilution experiments. Pronounced effects of sample grinding on the sharpness of the transition and on the form of the hysteresis curve were found, e.g., for [Fe(4,7-$(CH_3)_2$-phen)$_2$(NCS)$_2$]·α-picoline.[57] With increasing intensity of grinding, the transition assumes a quasi-continuous appearance, while the hysteresis loop becomes increasingly more narrow, and the residual fractions of both spin states increase dramatically (cf. Figure 7). The effect of metal dilution has been studied in the mixed-crystal series [Fe$_x$M$_{1-x}$(phen)$_2$(NCS)$_2$] where M = Mn^{2+}, Co^{2+}, Ni^{2+}, Zn^{2+}.[68] Starting from the abrupt transition in [Fe(phen)$_2$(NCS)$_2$] for x = 1.0, the transition becomes more gradual, the lower the iron concentration, with concurrent increase in the residual HS fraction at low temperatures for M = Mn^{2+}, and with increase in both the residual HS and LS fractions for M = Co^{2+}. Recently, grinding experiments on [Fe(phen)$_2$(NCS)$_2$] were also reported,[60] results similar to those discussed above for the α-picoline solvate of [Fe(4,7-$(CH_3)_2$-phen)$_2$(NCS)$_2$] having been obtained. Finally, the same applies to the detailed grinding and dilution studies on the HS ⇌ LS transition in the iron(III) complex [Fe(3-OCH_3-SalEen)$_2$]PF_6 where 3-OCH_3-SalEen is the monoanion of the condensation product of 3-methoxysalicylaldehyde and ethylenediamine.[69]

Recently, Müller et al.[50] investigated scanning curves of untreated and thoroughly ground samples of [Fe(bt)$_2$(NCS)$_2$]. It was demonstrated that, for the ground sample, the areas enclosed by two scanning curves were considerably different. Based on the Everett model it was concluded that domains in the mechanically treated sample are no longer independent and that interaction between neighboring domains takes place in the course of the HS ⇌ LS transition. Although a drastic reduction of domain size is again emphasized, this reduction may only partly be due to the grinding as such, whereas a heavy damage of the long-range order of the crystal lattice is believed to occur in addition. It should be noted that magnetic susceptibility clearly showed hysteresis effects which demonstrates that the spin transition has nonetheless preserved its first-order character.

E. General Conclusions

Evidently, a significant number of corresponding observations has been accumulated concerning abrupt HS ⇌ LS transitions, particularly those of iron(II) complexes. The results fit nicely into a more general description of these transitions. Thus, spin transitions of the discontinuous type show, in the transition region, pronounced domain formation by both the majority and minority phases. *The transition takes place by the conversion of independent domains of a particular spin state.* This process is favored over the individual spin conversion of a large number of isolated molecules; since the molar energy of isolated molecules distributed at random in the majority phase is larger than the molar energy of the domains of like spin. The size of the domains is limited in various ways.[45] For one, grain boundaries, cracks and dislocations in the crystal may determine the domain size. Furthermore, if the phase

conversion is accompanied by a change in volume, as has been clearly demonstrated for a number of spin transitions in complexes of iron(II),[27-30] the formation of the new phase will create local strains in the surroundings which will oppose any further growth of the domain. The transition is then self-quenching[45] in that each nucleus leads only to the conversion of a small domain. The Everett model does not provide means to determine the actual size of the domains. However, *individual X-ray diffraction patterns for the two phases, high-spin $^5T_2$ and low-spin $^1A_1$, are observed* in all examples discussed above. It follows that the domains formed should have at least the size of crystallites that yield sharp reflections in X-ray diffraction. The formation of isolated molecules of the new phase will be of importance in the beginning of a spin transition. Cooperative fluctuations[45] may carry neighboring molecules over the energy barrier separating the two spin states thus forming a nucleus of the new phase. As soon as the nucleus has achieved a critical size for which the energy is lower than the energy of the surrounding metastable phase, the nucleus will spontaneously grow until the complete domain has been converted. The experimental results show moreover that *the transition is associated with a crystallographic phase change* and that, in general, it is *thermodynamically first order.* Based on the Everett model it should be obvious that the hysteresis effects are a consequence of the domain formation. Thus it seems reasonable to assume that discontinuous type spin transitions arise for compounds with a strong cooperative interaction between the individual complexes.

With respect to particle size effects, it may be concluded that the change of a discontinuous type of transition, on grinding or doping the sample, into a transition showing a quasi-continuous behavior is essentially a consequence of the smaller size of the crystallites which are formed. For the smaller crystallites, the cooperative process will be terminated after a much shorter distance than in the original sample and this will result in a decreased size of domains and a more gradual appearance of the transition. The same smearing out of the transition may arise as result of an increased number of defects in the solid. The essential properties of the first-order transition, such as hysteresis effects, are nevertheless retained.

V. Continuous Transitions

A. Background

Continuous transitions may be described in terms of a gradual change with temperature of the relevant physical properties. Of considerable importance is the fact that, in the transition region, X-ray diffraction patterns reveal only a continuous shift of Bragg reflections with temperature. The resulting shift of lattice spacings shows an analogy to the variation of the high-spin fraction n_{HS}, as derived, e.g., from ^{57}Fe Mössbauer effect data. Beyond the transition region, a smaller increase of lattice spacings with increasing temperature is observed which is due to the normal thermal expansion of the lattice. A crystallographic phase change is not involved and thus the transition extends, in general, over a wide range of temperature.

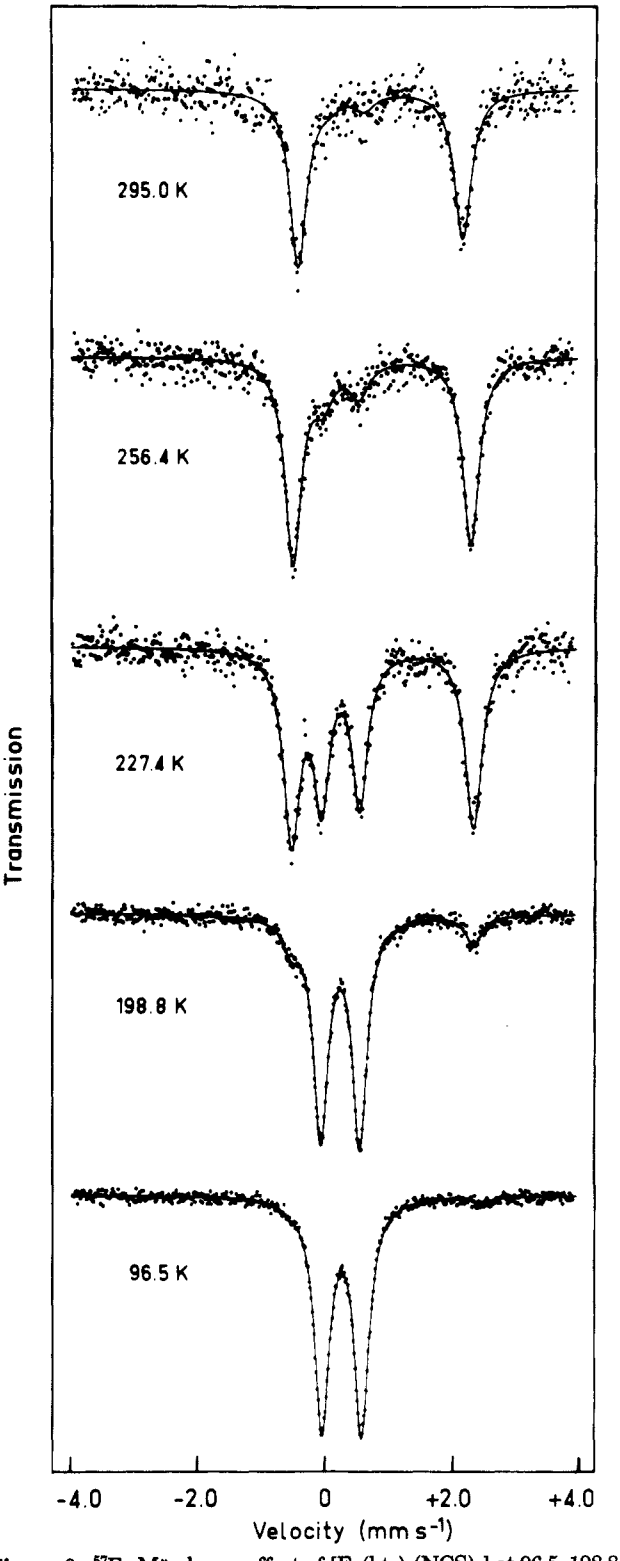

Figure 8. ^{57}Fe Mössbauer effect of $[Fe(bts)_2(NCS)_2]$ at 96.5, 198.8, 227.4, 256.4, and 295.0 K. The transition is centered at $T_c \simeq 219.5$ K.

The characteristic transition temperature T_c is therefore not as well defined as for discontinuous transitions. A latent heat of transition and hysteresis effects are equally not observed.

The number of systems showing a continuous type of spin transition is much larger than that showing a discontinuous transition. In the following, we restrict our attention to compounds where the particular physical data required to define the nature of the transition are available.

B. Specific Examples

$[Fe(bts)_2(NCS)_2]$. The compound where bts = 2,2′-bi(5-methyl-2-thiazoline) shows, on the basis of the ^{57}Fe Mössbauer effect, a continuous type high-spin ($^5T_2$) $\rightleftharpoons$ low-spin ($^1A_1$) transition centered at $T_c \simeq 219.5$ K.[62,70] Figure 8 shows a number of spectra which illustrate the development of the transition with temperature. Hysteresis effects were not observed. The temperature dependence of $-\ln(\sum t_i)$ where t_i is the effective thickness ($i = {}^5T_2, {}^1A_1$) shows a nonlinear behavior consistent with different Debye–Waller factors for the two spin constituents (cf. Figure 9). In contrast to the discontinuous type of transition, a single X-ray diffraction pattern is observed, the individual peaks showing a systematic shift of their positions with temperature. This is demonstrated in Figure 10 for two intense Bragg reflections. The values of lattice spacings d_{hkl} calculated from the line positions display a temperature dependence which goes parallel to that of $n_{^5T_2}$ derived from the Mössbauer effect, cf. Figure 11. From the results, it was concluded that the behavior of the system is similar to that of a solid solution of two spin isomers within the same lattice.[70]

$[Fe(4\text{-}paptH)_2](ClO_4)_2 \cdot 2H_2O$. The iron(II) complex of the tridentate NNN ligand (4-paptH = 2-((4-methyl-2-pyridyl)amino)-4-(2-pyridyl)thiazole) shows a continuous high-spin($^5T_2$) $\rightleftharpoons$ low-spin($^1A_1$) transition, whereby $T_c \simeq 185$ K.[71,72] The transition is incomplete with significant residual $^5T_2$ and $^1A_1$ fractions at the corresponding temperature ends. The quantity $-\ln(\sum t_i)$ shows a nonlinear temperature dependence which indicates different Debye–Waller factors for the two spin states, cf. Figure 9. The X-ray powder diffraction shows a single pattern, the temperature function of the lattice spacings d_{hkl} being analogous to that of $n_{^5T_2}$. The results for the complex tetrafluoroborate, $[Fe(4\text{-}paptH)_2](BF_4)_2 \cdot 2H_2O$, are closely similar to those for the perchlorate, the transition being centered at $T_c \simeq 220$ K.[72]

$[Fe(dppen)_2Cl_2] \cdot 2(CH_3)_2CO$. For this complex of a PP ligand (dppen = *cis*-1,2-bis(diphenylphosphino)-ethylene), a continuous high-spin($^5T_2$) $\rightleftharpoons$ low-spin($^1A_1$) transition was observed on the basis of magnetic susceptibility, optical spectra, and X-ray diffraction.[30] Detailed studies of the temperature dependence of the ^{57}Fe Mössbauer effect and X-ray powder diffraction produced results similar to the examples discussed above.[23] The transition is centered at $T_c \simeq 240$ K and hysteresis effects are not involved. A single X-ray powder diffraction pattern is observed, the lattice spacings d_{hkl} showing a continuous shift with temperature. Independent single-crystal X-ray diffraction studies at the temperatures of 295 and 130 K established that there is no change of space group in the course of the transition.[30] The line widths of the Mössbauer spectra show an unusual increase at about 240 K, additional anomalies being encountered for $\Delta E_Q(^5T_2)$ and $t_{^5T_2}/t_{total}$. The effect has been attributed to an order–disorder transition of the acetone molecules which affects the Mössbauer spectra via change of the Fe–P ligation.

$[Fe(4\text{-}CH_3\text{-}phen)_2(NCS)_2]$. Magnetic susceptibility and ^{57}Fe Mössbauer effect measurements indicate[73] that the compound exhibits a continuous type high-spin($^5T_2$) $\rightleftharpoons$ low-spin($^1A_1$) transition at $T_c = 215$ K without hysteresis. Different Debye–Waller factors are again suggested by the nonlinear temperature function of $-\ln$

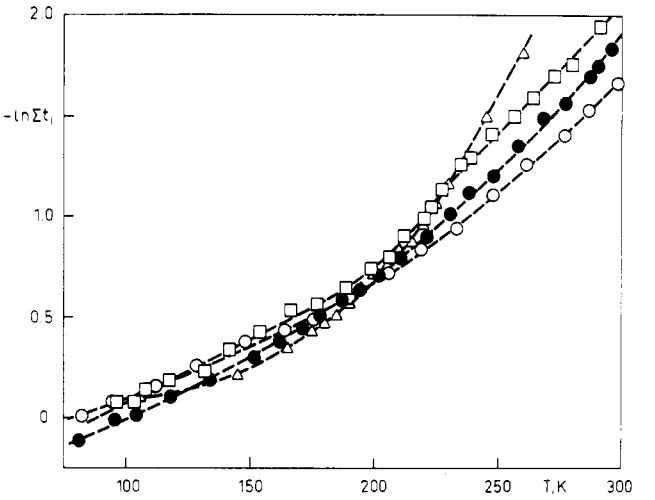

Figure 9. Temperature dependence of the quantity $-\ln(\sum t_i)$, $i = {}^5T_2, {}^1A_1$, where t_i is the effective thickness, on the basis of ^{57}Fe Mössbauer effect measurements for $[Fe(bts)_2(NCS)_2]$ (□), $[Fe(4\text{-}paptH)_2](ClO_4)_2 \cdot 2H_2O$ (●), $[Fe(4\text{-}paptH)_2](BF_4)_2 \cdot 2H_2O$ (○), and $[Fe(4\text{-}CH_3\text{-}phen)_2(NCS)_2]$ (△).

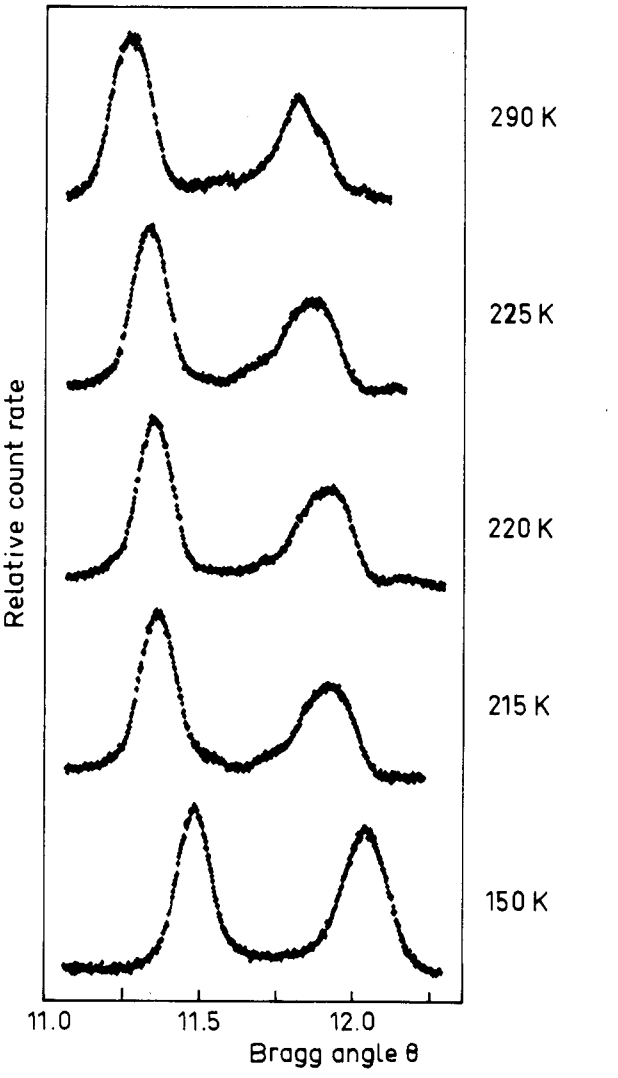

Figure 10. X-ray diffraction peak profiles for two intense Bragg reflections of $[Fe(bts)_2(NCS)_2]$ at a number of temperatures.

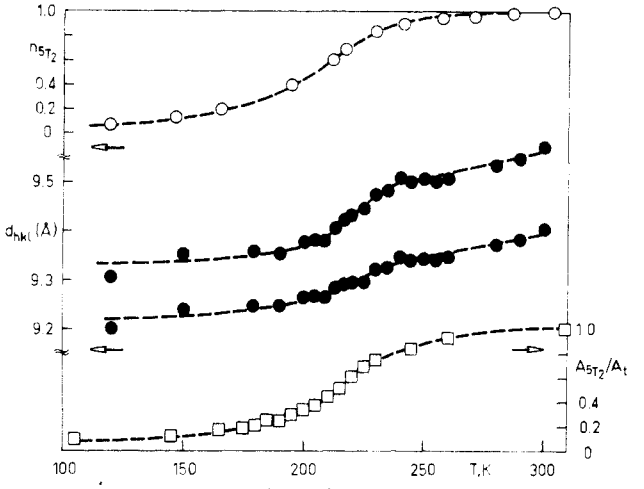

Figure 11. Temperature dependence of the lattice spacings d_{hkl} for two Bragg reflections and the $^5T_2$ fraction $n_{^5T_2}$ from the Mössbauer effect of $[Fe(bts)_2(NCS)_2]$.

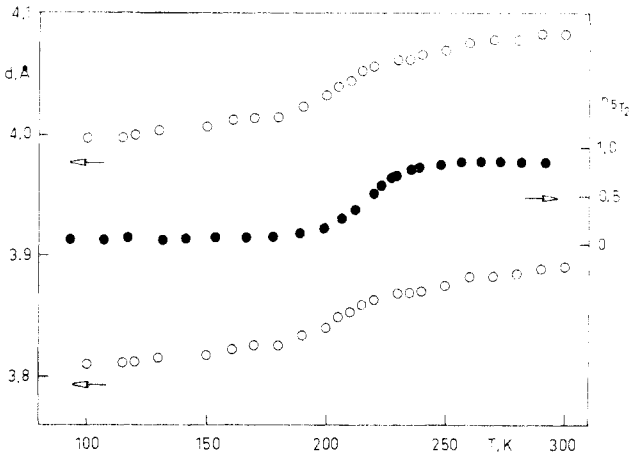

Figure 12. Temperature dependence of the lattice spacings d_{hkl} for two Bragg reflections (●), the $^5T_2$ fraction $n_{^5T_2}$ from magnetism (○), and the area ratio $A_{^5T_2}/A_{total}$ from the Mössbauer effect (□) of $[Fe(4\text{-}CH_3\text{-}phen)_2(NCS)_2]$.

($\sum t_i$), cf. Figure 9. X-ray powder diffraction studies between 120 and 300 K[74] revealed a single diffraction pattern in the spin transition region. The temperature dependence of the interplanar separations corresponding to two selected Bragg reflections is displayed in Figure 12 in conjunction with the values of $n_{^5T_2}$ derived from magnetic studies and the ratio $t_{^5T_2}/t_{total}$ obtained from the Mössbauer effect areas. Obviously, all these quantities show a similar behavior.

[Fe(pythiaz)$_2$](BF$_4$)$_2$. The iron(II) complex of the tridentate ligand pythiaz = 2,4-bis(2-pyridyl)thiazole shows a continuous type high-spin($^5T_2$) ⇌ low-spin($^1A_1$) transition with a high residual $^5T_2$ fraction at low temperatures, as demonstrated by magnetic and ^{57}Fe Mössbauer effect studies.[75] The transition takes place at $T_c \simeq 173$ K, if the residual fraction is accounted for. Again, the interplanar separations from X-ray diffraction,[74] the $n_{^5T_2}$ values from magnetism, and the area fractions $A_{^5T_2}/A_{total}$ from Mössbauer effect measurements show an analogous temperature dependence thus confirming the interrelation of these properties.

[Fe(2-pic)$_3$]Cl$_2$·CH$_3$OH. The complex where 2-pic = 2-picolylamine shows, on the basis of magnetic[76] and ^{57}Fe Mössbauer effect studies,[65] a continuous type high-spin ($^5T_2$) ⇌ low-spin ($^1A_1$) transition centered at

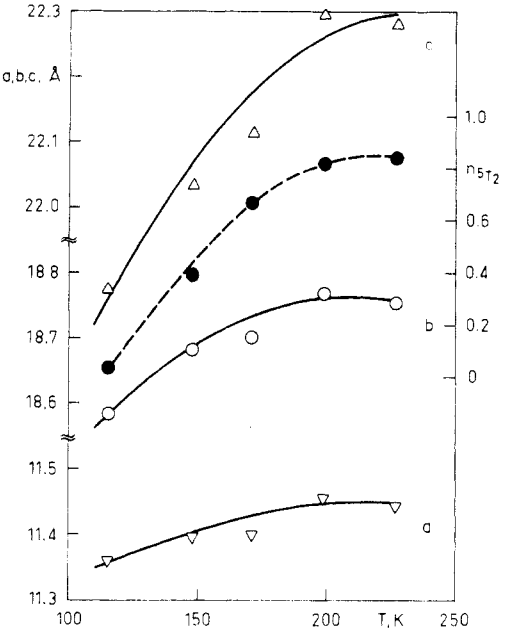

Figure 13. Temperature dependence of the lattice constants a, b, c, and the $^5T_2$ fraction $n_{^5T_2}$ (●) on the basis of a single-crystal X-ray diffraction study of $[Fe(2\text{-}pic)_3]Cl_2\cdot CH_3OH$ (according to Katz and Strouse[28]). The values at 171 K have not been included in the numerical fit.

$T_c \simeq 153$ K. No hysteresis effects have been encountered. Of great significance is a variable-temperature single-crystal X-ray diffraction study.[28] The compound crystallizes in the orthorhombic space group *Pbna*, $Z = 4$, and $a = 11.359$ Å, $b = 18.582$ Å, $c = 21.873$ Å at 115 K. Figure 13 illustrates the reported dependence on temperature for the lattice constants a, b, c and for the high-spin fraction $n_{^5T_2}$. It may be easily seen that a, b, and c show an increase proportional to $n_{^5T_2}$ as expected from Vegard's law. This result is direct evidence that, in the transition region, the system shows a behavior similar to that of a random solid solution of the two-spin isomers.

C. Additional Comments

The considerable number of iron(II) compounds where the apparently continuous high-spin ($^5T_2$) ⇌ low-spin ($^1A_1$) transition has not been studied in any great detail is not discussed here. Even for a complex such as $[Fe(2\text{-}pic)_3]Cl_2\cdot C_2H_5OH$, some conflicting results exist. The pure compound shows a transition at $T_c = 121.5$ K, no hysteresis effects having been observed.[43] An exhaustive ^{57}Fe Mössbauer effect study of the series of diluted complexes $[Fe_xZn_{1-x}(2\text{-}pic)_3]Cl_2\cdot C_2H_5OH$ has revealed a systematic variation of the transition temperature with composition.[43,77] A single-crystal X-ray diffraction study of $[Fe(2\text{-}pic)_3]Cl_2\cdot C_2H_5OH$ has been carried out at 298, 150, and 90 K.[29] The compound crystallizes in the monoclinic space group $P2_1/c$, $Z = 4$ and $a = 11.831$ Å, $b = 22.021$ Å, $c = 11.551$ Å, $\beta = 124.28°$ at 298 K. It was concluded that no change of space group is involved. However, the lattice constants a and b show small though abrupt changes in the transition region,[29] and there is a report on a significant change of a to 10.768 Å at 115 K.[28] This change is reflected in a pronounced anomaly of Mössbauer and

magnetic susceptibility data in the region between 114 and 120.7 K.[78] In addition, Mikami et al.[29] observed an order–disorder transition of the ethanol solvate molecule which is believed to trigger the spin conversion in $[Fe(2\text{-pic})_3]Cl_2 \cdot C_2H_5OH$. It should be noted that a similar order–disorder transition of the acetone molecule was encountered for $[Fe(dppen)_2Cl_2] \cdot 2(CH_3)_2CO$, although no implication on the character of the spin transformation was apparent.[23] In $[Fe(2\text{-pic})_3]Cl_2 \cdot C_2H_5OH$, however, the dilution experiments are indicative of a significant degree of cooperativity, the average domain size having been calculated to between $n \approx 3.5$[79] and $n \approx 500$.[29] Of course, many real transformations are of mixed order[35] and, indeed, it has been suggested that the transition in $[Fe(2\text{-pic})_3]Cl_2 \cdot C_2H_5OH$ should be considered as having a first- and second-order component. Due to these complications, it is assumed that,, for the present purpose, the nature of the transition in this compound is not definitely settled.

D. General Conclusions

It seems that a significant amount of consistent results has been collected on compounds which show continuous type spin transitions, especially those of iron(II). The characteristic properties of these transitions are the *nonexistence of a crystallographic phase change and the absence of hysteresis effects.* Both phenomena, if encountered, are the consequence of domain formation. It has therefore been concluded that, for continuous type spin transitions, domains play a minor role and, consequently, these transitions will be encountered preferentially for compounds with a weak cooperative interaction. This inference may be illustrated by an estimate of domain size for a compound showing a discontinuous spin transition as compared to that for a continuous transition. As mentioned above, the number of molecules per domain in $[Fe(phen)_2(NCS)_2]$ has been obtained as $n \approx 90$,[24] whereas for $[Fe(2\text{-pic})_3]Cl_2 \cdot C_2H_5OH$ the estimate is $n \approx 3.5$.[79]

Moreover, the experimental results indicate that, for continuous type spin transitions, the two spin isomers show a behavior which is similar to that of a solid solution of two components. In general, solid solutions are formed if the two pure phases are isomorphous, if the atomic radii of the involved atoms (e.g., for alloys) do not differ by more than about 10%, and if the distribution of the two phases is at random.[34,80] In the present context, the similarity to a solid solution is established by a material in which equivalent sites are occupied at random by molecules of the two spin species, in continuously variable proportions governed by the temperature.[81] This material will show a single set of physical properties intermediate between those of the two pure spin constituents. It is evident that the examples for continuous type spin transitions presented above do show just this type of behavior.

VI. A Simple Model and Some Considerations Concerning Both Types of Transition

The above results may be nicely interpreted in terms of a model which derives from regular solution theory.[82] When the method of Slichter and Drickamer[83] was used, the molar Gibbs free energy for a mixture of HS and LS molecules may be written as

$$G = n_{HS}G_{HS} + (1 - n_{HS})G_{LS} + \Gamma n_{HS}(1 - n_{HS}) - TS_{mix} \quad (10)$$

Here, G_{HS} and G_{LS} is the Gibbs free energy per mole of HS and LS molecules, respectively, and n_{HS} is the fraction of HS molecules in the crystal. In addition, Γ is an interaction term according to which the free energy of formation is dependent on the spin-state conversion of neighboring ions and S_{mix} is the mixing entropy of the HS and LS molecules in the lattice

$$S_{mix} = k[n_{HS} \ln n_{HS} + (1 - n_{HS}) \ln (1 - n_{HS})] \quad (11)$$

At equilibrium

$$\left(\frac{\partial G}{\partial n_{HS}}\right)_{p,T} = 0 \quad (12)$$

and thus

$$kT \ln \left(\frac{1 - n_{HS}}{n_{HS}}\right) = \Delta G + \Gamma(1 - 2n_{HS}) \quad (13)$$

where $\Delta G = G_{HS} - G_{LS}$. Equation 13 may be conveniently rewritten as

$$\ln \left(\frac{1 - n_{HS}}{n_{HS}}\right) = \frac{\Delta H + \Gamma(1 - 2n_{HS})}{kT} - \frac{\Delta S}{k} \quad (14)$$

This equation may be solved easily by graphical methods. Provided that the quantities ΔH, ΔS, and Γ are known, n_{HS} may be determined for each temperature by intersecting the curve $\ln [(1 - n_{HS})/n_{HS}]$ with the straight line of slope $-2\Gamma/kT$ through the point $P(^1/_2 + \Delta H/2\Gamma; -\Delta S/k)$.[84] For $\Gamma < 2kT_c$ a unique solution for each particular temperature is found. This situation corresponds to a single minimum of the Gibbs free energy G and thus to a gradual temperature dependence of n_{HS} ("continuous spin transition"). If $\Gamma = 2kT_c$, the slope of the straight line equals that of the central region of the logarithmic curve. Again a unique solution of eq 14 is obtained, although there is a jump of n_{HS} at T_c associated with a vertical turning tangent ("discontinuous spin transition"). Finally, for $\Gamma > 2kT_c$ three solutions are found at each temperature between $T_c^{\uparrow}$ and $T_c^{\downarrow}$, two values of n_{HS} corresponding to minima of G, the intermediate third value representing a system out of equilibrium. Thus abrupt changes of n_{HS} result for rising as well as for lowering of temperature at $T_c^{\uparrow}$ and $T_c^{\downarrow}$, respectively ("discontinuous spin transition with hysteresis"). This model has been applied for a qualitative interpretation of discontinuous as well as continuous transitions. An example of a discontinuous transition is provided by the study of hysteresis effects in $[Fe(4,7\text{-}(CH_3)_2\text{-phen})_2(NCS)_2]$.[54] In case of continuous transitions, the model has been implemented by taking into account the volume change[27,28,29] associated with the HS $\rightleftharpoons$ LS transition. This modification has been achieved on the basis of the theory of elastic interactions.[85] The model is then capable of reproducing the temperature dependence of n_{HS} for different concentrations x of the iron atom in $[Fe_xZn_{1-x}(2\text{-pic})_3]Cl_2 \cdot C_2H_5OH$ as well as the dependence of the critical temperature T_c on x in the same series of compounds.[85] More recently, a similar study of metal dilution effects has been reported for the corresponding cobalt host lattice.[86] Thus a quantitative interpretation of the continuous type HS $\rightleftharpoons$ LS transitions has been

achieved, whereas, for discontinuous transitions, this is not easily possible. Certain properties of the solid, such as the size and growth of domains, which determine the detailed form of these transitions can be accounted for alone by a theory like the Everett model[44-47] discussed above. In fact, the basic difference between the two types of transition is believed to be due to the distribution of the two spin phases in the lattice. The differentiation is derived from the experimental findings in X-ray diffraction: a *narrow distribution* is defined by the formation of domains of the minority phase which exceed the critical size of $\simeq$1000 Å[80] required in order to produce an individual diffraction pattern; a *wide distribution* involves smaller domains or no domains at all and does therefore not become manifest in X-ray diffraction. The diffraction results thus suggest that, for continuous transitions, a wide distribution of the minority spin phase within the majority phase should be assumed, whereas for discontinuous transitions, a narrow distribution of the two phases has been established.

Finally, it is believed that in both cases discussed here, i.e., the discontinuous and continuous type spin transitions, the conversion of spin state will be initiated in much the same way. Homogeneous nucleation is known to be caused by thermal fluctuations and follows VWBD theory.[87,88] However, since perfectly homogeneous nucleation almost never occurs, formation of nuclei of the product phase will start at defect sites, on the surface, at grain boundaries and other locations of relatively high energy. Moreover, the specific volumes of the parent and the product phase are different[27-29] and hence lattice strains will develop because of disregistry across the surface. The differentiation between the two types of transition seems to arise in the course of further development of the nuclei. For discontinuous transitions, a limited number of nuclei will show preferred growth with change of temperature and, eventually, the overwhelming part of the parent phase will transform into the product phase at T_c. For continuous transitions, the growth of nuclei must be retarded in some way and thus the formation of new nuclei of the product phase will continue until all of the material has been gradually converted.

The different volumes of the HS and LS phase are a consequence of different Fe–ligand distances and some small changes of molecular geometry.[27-29] Associated herewith are changes of intramolecular vibrations[89,90] and these cause the difference in recoil-free fraction which is consistently encountered for the two spin phases in both the discontinuous and continuous type HS $\rightleftharpoons$ LS transitions.

VII. Residual High-Spin and Low-Spin Fractions

In various iron(II) complexes showing a high-spin($^5T_2$) $\rightleftharpoons$ low-spin($^1A_1$) transition, the HS-fraction levels out to a more or less constant value in the lower temperature range, forming what has been called the residual paramagnetic fraction. In some cases, particularly as the result of grinding and doping experiments, a residual diamagnetic, i.e., $^1A_1$ fraction, may be equally formed at the high temperatures. For the general case of a HS $\rightleftharpoons$ LS transition, the relevant quantities should be called the residual HS- and residual LS-fraction, respectively.

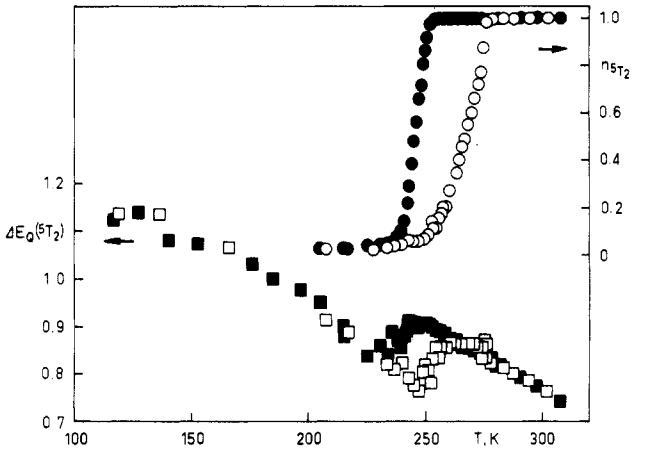

Figure 14. Temperature dependence of the quadrupole splitting of the $^5T_2$ phase $\Delta E_Q(^5T_2)$ and the $^5T_2$ fraction $n_{^5T_2}$ for [Fe(phy)$_2$](ClO$_4$)$_2$. Open signs refer to measurements for increasing temperatures; solid signs correspond to decreasing temperatures.

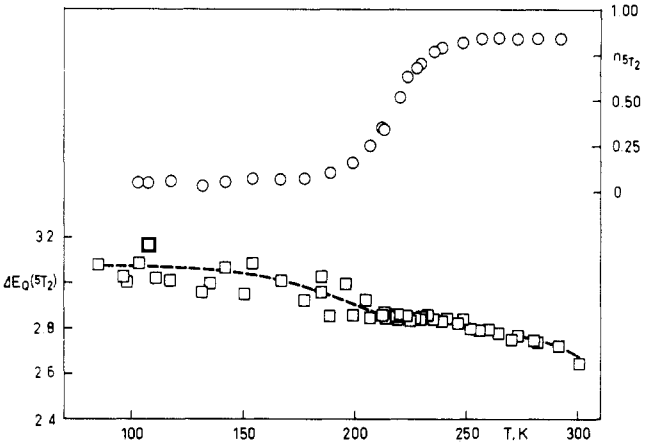

Figure 15. Temperature dependence of the quadrupole splitting of the $^5T_2$ isomer $\Delta E_Q(^5T_2)$ (□) and the $^5T_2$ fraction $n_{^5T_2}$ (○) for [Fe(bts)$_2$(NCS)$_2$].

Recently, a pronounced discontinuity in the temperature dependence of the ^{57}Fe Möessbauer quadrupole splitting $\Delta E_Q(^5T_2)$ has been found for the discontinuous type spin transition in [Fe(phy)$_2$](ClO$_4$)$_2$,[91] cf. Figure 14. It follows that the temperature function of $\Delta E_Q(^5T_2)$ for the residual $^5T_2$ fraction below T_c which amounts to about 3% is significantly different from that for the bulk $^5T_2$ phase above T_c. X-ray powder diffraction shows that, as illustrated by Figure 3, an individual peak profile for the residual $^5T_2$ phase may be still distinguished, e.g., at 243 K, where the $^1A_1$ phase is predominant (cf. arrows in Figure 3).

For the continuous type spin transition in [Fe(bts)$_2$(NCS)$_2$], a similar discontinuity in the values of $\Delta E_Q(^5T_2)$ has been observed in the region of T_c, as demonstrated by Figure 15.[91] On the other hand, the X-ray powder diffraction illustrated by Figure 10 shows only the shift of peak positions expected for a continuous transition, whereas no additional peaks are observed at low temperatures where $n_{^5T_2} \simeq 0.04$.

The results for [Fe(phy)$_2$](ClO$_4$)$_2$ may be easily rationalized. The molecules of the residual $^5T_2$ fraction form crystallites of the size $\approx$ 1000 Å or more since these are sufficiently large to give an individual X-ray diffraction pattern; although these crystallites are still too small to participate in the crystallographic phase change. The reason seems to be the enhanced surface energy of the crystallites. The same explanation as

suggested here should apply to the discontinuity of $\Delta E_Q(^5T_2)$ observed for precipitated samples of [Fe(phen)$_2$(NCS)$_2$],[59] since this material contains a residual $^5T_2$ fraction of about 12%.

Since in continuous type spin transitions, such as in the compound [Fe(bts)$_2$(NCS)$_2$], no separate diffraction pattern for the residual $^5T_2$ fraction is found, the size of the crystallites cannot be responsible for the observations. For [Fe(bts)$_2$(NCS)$_2$] at low temperatures, $n_{^5T_2}$ is found to be only about 0.04. However, even for the iron(II) complexes [Fe(4-paptH)$_2$]X$_2$·2H$_2$O where X = ClO_4, BF_4 where the residual $^5T_2$ fraction is $n_{^5T_2} \simeq 0.20$,[72] no separate diffraction pattern has been obtained. For [Fe(bts)$_2$(NCS)$_2$], even the small crystallites which are produced by grinding of the sample are participating in the spin transition, since no individual X-ray diffraction pattern is found.[91] It has therefore been suggested that, for the continuous type HS ⇌ LS transitions, the residual $^5T_2$ molecules are trapped within the lattice at some kind of defect. The two spin isomers are known to show a volume difference.[27-29] Consequently, the residual $^5T_2$ molecules which are located at a lattice site of the bulk $^1A_1$ phase will be under compression, and this situation will produce a change of the $\Delta E_Q(^5T_2)$ values as observed. The interpretation is consistent with the assumption that essentially no domains are participating in this type of transition.

Acknowledgments. We appreciate financial support by the Deutsche Forschungsgemeinschaft and the Stiftung Volkswagenwerk. We are grateful to H. A. Goodwin and T. Waigel for reading the manuscript and for their comments.

VIII. References and Notes

(1) König, E. *Ber. Bunsenges. Phys. Chem.* **1972**, *76*, 975.
(2) Goodwin, H. A. *Coord. Chem. Rev.* **1976**, *18*, 293.
(3) Gütlich, P. *Adv. Chem. Ser.* **1981**, *No. 194*, 405.
(4) Gütlich, P. *Struct. Bonding* **1981**, *44*, 83.
(5) Martin, R. L.; White, A. H. *Transition Met. Chem. (N.Y.)* **1968**, *4*, 113.
(6) König, E.; Kremer, S. *Theor. Chim. Acta* **1971**, *23*, 12.
(7) However, as soon as an individual complex changes from LS to HS or vice versa, the crystal field energy changes in accordance with the associated geometrical distortion of the molecule, cf. section III. Therefore, the attempt at a direct determination of the critical crystal field strength of eq 1 based on experimental results is fortuitous.
(8) Dose, E. V.; Hoselton, M. A.; Sutin, N.; Tweedle, M. F.; Wilson, L. J. *J. Am. Chem. Soc.* **1978**, *100*, 1141.
(9) Bari, R. A.; Sivardière, J. *Phys. Rev. B: Condens. Matter* **1972**, *5*, 4466.
(10) Zimmermann, R.; König, E. *J. Phys. Chem. Solids* **1977**, *38*, 779.
(11) Gütlich, P.; Köppen, H.; Link, R.; Steinhäuser, H. G. *J. Chem. Phys.* **1979**, *70*, 3977.
(12) Rao, P. S.; Ganguli, P.; McGarvey, B. R. *Inorg. Chem.* **1981**, *20*, 3682.
(13) Kambara, T. *J. Chem. Phys.* **1979**, *70*, 4199.
(14) Kambara, T. *J. Chem. Phys.* **1981**, *74*, 4557.
(15) Bhide, V. G.; Rajoria, D. S.; Rama Rao, G.; Rao, C. N. R. *Phys. Rev. B* **1972**, *6*, 1021.
(16) Bose, M.; Ghoshray, A.; Basu, A.; Rao, C. N. R. *Phys. Rev. B: Condens. Matter* **1982**, *26*, 4871.
(17) Imoto, H.; Simon, A. *Inorg. Chem.* **1982**, *21*, 308.
(18) Iizuka, T.; Yonetani, T. *Adv. Biophys.* **1970**, *1*, 157.
(19) Tamura, M. *Biochim. Biophys. Acta* **1971**, *243*, 249.
(20) Yonetani, T.; Iizuka, T.; Asakura, T. *J. Biol. Chem.* **1972**, *247*, 863.
(21) König,, E.; Kremer, S. "Ligand Field Energy Diagrams"; Plenum Press: New York, 1977.
(22) König, E.; Ritter, G.; Kulshreshtha, S. K.; Nelson, S. M. *Inorg. Chem.* **1982**, *21*, 3022.
(23) König, E.; Ritter, G.; Kulshreshtha, S. K.; Waigel, J.; Sacconi, L. *Inorg. Chem.* **1984**, *23*, 1241.
(24) Sorai, M.; Seki, S. *J. Phys. Chem. Solids* **1974**, *35*, 555.
(25) Kulshreshtha, S. K.; Iyer, R. M.; König, E.; Ritter, G. *Chem. Phys. Lett.* **1984**, *110*, 201.
(26) Kulshreshtha, S. K.; Iyer, R. M. *Chem. Phys. Lett.* **1984**, *108*, 501.
(27) König, E.; Watson, K. J. *Chem. Phys. Lett.* **1970**, *6*, 457.
(28) Katz, B. A.; Strouse, C. E. *J. Am. Chem. Soc.* **1979**, *101*, 6214.
(29) Mikami, M.; Konno, M.; Saito, Y. *Acta Crystallogr., Sect. B* **1980**, *B36*, 275.
(30) Cecconi, F.; DiVaira, M.; Middollini, S.; Orlandini, A.; Sacconi, L. *Inorg. Chem.* **1981**, *20*, 3423.
(31) Ehrenfest, P. *Proc. Amsterdam Acad.* **1933**, *36*, 153.
(32) Ubbelohde, A. R. *Quart. Rev. (London)* **1957**, *11*, 246.
(33) Zimmermann, R. *J. Phys. Chem. Solids* **1983**, *44*, 151.
(34) Megaw, H. D., "Crystal Structures: A Working Approach"; W. B. Saunders: Philadelphia, 1973.
(35) Rao, C. N. R.; Rao, K. J., "Phase Transitions in Solids"; McGraw-Hill: New York, 1978.
(36) Smoluchowski, R.; Mayer, J. E.; Weyl, W. A., "Phase Transformations in Solids"; Wiley: New York, 1951.
(37) Vos, G.; De Graaf, R. A. G.; Haasnoot, J. G.; Van Der Kraan, A. M.; De Vaal, P.; Reedijk, J. *Inorg. Chem.* **1984**, *23*, 2905.
(38) Stahl, K. *Acta Crystallogr., Sect. B* **1983**, *B39*, 612.
(39) Leipoldt, J. G.; Coppens, P. *Inorg. Chem.* **1973**, *12*, 2269.
(40) Scheidt, W. R.; Geiger, D. K.; Haller, K. J. *J. Am. Chem. Soc.* **1982**, *104*, 495.
(41) Haller, K. J.; Johnson, P. L.; Feltham, R. D.; Enemark, J. H.; Ferraro, J. R.; Basile, L. J. *Inorg. Chim. Acta* **1979**, *33*, 119.
(42) Irler, W.; Ritter, G.; König, E.; Goodwin, H. A.; Nelson, S. M. *Solid State Commun.* **1979**, *29*, 39.
(43) Sorai, M.; Ensling, J.; Gütlich, P. *Chem. Phys.* **1976**, *18*, 199.
(44) Everett, D. H.; Smith, F. W. *Trans. Faraday Soc.* **1954**, *50*, 187.
(45) Everett, D. H.; Whitton, W. I. *Trans. Faraday Soc.* **1952**, *48*, 749.
(46) Everett, D. H. *Trans. Faraday Soc.* **1954**, *50*, 1077; **1955**, *51*, 1551.
(47) Enderby, J. A. *Trans. Faraday Soc.* **1955**, *52*, 106.
(48) König, E.; Ritter, G.; Irler, W.; Goodwin, H. A. *J. Am. Chem. Soc.* **1980**, *102*, 4681.
(49) In general, the starting points on the increasing branch of the hysteresis loop are not equal in temperature. For the present case of the [Fe(phy)$_2$](ClO$_4$)$_2$ complex,[48] this difference is within the experimental uncertainty of temperature reading and is thus negligible. The statement by Müller et al.[50] that the inner loops in our study[48] were not scanned between the same temperatures as required by the Everett model therefore does not apply.
(50) Müller, E. W.; Spiering, H.; Gütlich, P. *J. Chem. Phys.* **1983**, *79*, 1439.
(51) König, E.; Ritter, G.; Kulshreshtha, S. K.; Waigel, J.; Goodwin, H. A. *Inorg. Chem.* **1984**, *23*, 1896.
(52) König, E.; Kanellakopulos, B., to be published.
(53) König, E.; Ritter, G.; Waigel, J.; Goodwin, H. A. *J. Chem. Phys.*, in press.
(54) König, E.; Ritter, G. *Solid State Commun.* **1976**, *18*, 279.
(55) König, E.; Ritter,, G.; Irler, W. *Chem. Phys. Lett.* **1979**, *66*, 336.
(56) König, E.; Ritter, G.; Kanellakopulos, B. *J. Phys. C* **1974**, *7*, 2681.
(57) König, E.; Ritter, G.; Kulshreshtha, S. K.; Csatary, N. *Inorg. Chem.* **1984**, *23*, 1903.
(58) König, E.; Madeja, K. *Inorg. Chem.* **1967**, *6*, 48.
(59) Ganguli, P.; Gütlich, P.; Müller, E. W.; Irler, W. *J. Chem. Soc., Dalton Trans.* **1981**, 441.
(60) Müller, E. W.; Spiering, H.; Gütlich, P. *Chem. Phys. Lett.* **1982**, *93*, 567.
(61) König, E.; Madeja, K.; Watson, K. J. *J. Am. Chem. Soc.* **1968**, *90*, 1146.
(62) Bradley, G.; McKee, V.; Nelson, S. M.; Nelson, J. *J. Chem. Soc., Dalton Trans.* **1978**, 522.
(63) König, E.; Ritter, G.; Irler, W.; Nelson, S. M. *Inorg. Chim. Acta* **1979**, *37*, 169.
(64) Burnett, M. G.; McKee, V.; Nelson, S. M. *J. Chem. Soc., Dalton Trans.* **1981**, 1492.
(65) Sorai, M.; Ensling, J.; Hasselbach, K. M.; Gütlich, P. *Chem. Phys.* **1977**, *20*, 197.
(66) Ritter, G.; König, E.; Irler, W.; Goodwin, H. A. *Inorg. Chem.* **1978**, *17*, 224.
(67) Wells, F. V.; McCann, S. W.; Wickman, H. H.; Kessel, S. L.; Hendrickson, D. N.; Feltham, R. D. *Inorg. Chem.* **1982**, *21*, 2306.
(68) Ganguli, P.; Gütlich, P.; Müller, E. W. *Inorg. Chem.* **1982**, *21*, 3429.
(69) Haddad, M. S.; Federer, W. D.; Lynch, M. W.; Hendrickson, D. N. *Inorg. Chem.* **1981**, *20*, 131.
(70) König, E.; Ritter, G.; Kulshreshtha, S. K.; Nelson, S. M. *J. Am. Chem. Soc.* **1983**, *105*, 1924.
(71) Goodwin, H. A.; Mather, D. W. *Aust. J. Chem.* **1972**, *25*, 715.
(72) König, E.; Ritter, G.; Kulshreshtha, S. K.; Goodwin, H. A.

Inorg. Chem. **1983**, *22*, 2518.
(73) König, E.; Ritter, G.; Irler, W.; Kanellakopulos, B. *J. Phys. C* **1977**, *10*, 603.
(74) Irler, W. Ph.D. Thesis, University of Erlangen-Nürnberg, Erlangen, West Germany, 1979.
(75) König, E.; Ritter, G.; Goodwin, H. A. *Chem. Phys.* **1973**, *1*, 17.
(76) Greenaway, A. M.; Sinn, E. *J. Am. Chem. Soc.* **1978**, *100*, 8080.
(77) Gütlich, P.; Link, R.; Steinhäuser, H. G. *Inorg. Chem.* **1978**, *17*, 2509.
(78) Köppen, H.; Müller, E. W.; Köhler, C. P.; Spiering, H.; Meissner, E.; Gütlich, P. *Chem. Phys. Lett.* **1982**, *91*, 348.
(79) Gütlich, P.; Köppen, H.; Link, R.; Steinhäuser, H. G. *J. Chem. Phys.* **1979**, *70*, 3977.
(80) Bunn, C. W. "Chemical Crystallography"; Oxford University Press: London, 1961.
(81) Ohnishi, S.; Sugano, S. *J. Phys. C* **1981**, *14*, 39.
(82) Guggenheim, E. A., "Mixtures"; Oxford University Press: London, 1952.
(83) Slichter, C. P.; Drickamer, H. G. *J. Chem. Phys.* **1972**, *56*, 2142.
(84) Drickamer, H. G.; Frank, C. W. "Electronic Transitions and the High Pressure Chemistry and Physics of Solids"; Chapman and Hall: London, 1973.
(85) Spiering, H.; Meissner, E.; Köppen, H.; Müller,, E. W.; Gütlich, P. *Chem. Phys.* **1982**, *68*, 65.
(86) Sanner, I.; Meissner, E.; Köppen, H.; Spiering, H.; Gütlich, P. *Chem. Phys.* **1984**, *86*, 227.
(87) Volmer, M.; Weber, A. *Z. Phys. Chem.* **1925**, *119*, 277.
(88) Becker, R.; Döring, W. *Ann. Phys.* **1935**, *24*, 119.
(89) Takemoto, J. H.; Hutchinson, B. *Inorg. Nucl. Chem. Lett.* **1972**, *8*, 769.
(90) Takemoto, J. H.; Hutchinson, B. *Inorg. Chem.* **1973**, *12*, 705.
(91) König, E.; Ritter, G.; Kulshreshtha, S. K. *Inorg. Chem.* **1984**, *23*, 1144.